

# Reconfigurable Multiplexed Point of Care System for Monitoring Type 1 Diabetes Patients

Augusto Márquez,<sup>a</sup> Joan Aymerich,<sup>a</sup> Michele Dei,<sup>a</sup> Rosalía Rodríguez-Rodríguez,<sup>b</sup>  
Manuel Vázquez-Carrera,<sup>c</sup> Javier Pizarro-Delgado,<sup>c</sup> Pablo Giménez-Gómez,<sup>a</sup> Ángel  
Merlos,<sup>a</sup> Lluís Terés,<sup>a</sup> Francesc Serra-Graells,<sup>a</sup> Cecilia Jiménez-Jorquera,<sup>a</sup> Carlos  
Domínguez,<sup>a</sup> Xavier Muñoz-Berbel,<sup>a\*</sup>

<sup>a</sup> *Instituto de Microelectrónica de Barcelona, (IMB-CNM, CSIC), Bellaterra, Barcelona, Spain*

<sup>b</sup> *Basic Sciences Department, Faculty of Medicine and Health Sciences, Universitat Internacional de Catalunya, 08195 Sant Cugat del Vallès, Spain.*

<sup>c</sup> *Department of Pharmacology, Toxicology and Therapeutic Chemistry, Faculty of Pharmacy and Food Sciences, University of Barcelona; Institute of Biomedicine of the University of Barcelona (IBUB); Spanish Biomedical Research Center in Diabetes and Associated Metabolic Diseases (CIBERDEM)-Instituto de Salud Carlos III; Pediatric Research Institute-Hospital Sant Joan de Déu, Barcelona, Spain.*

\* Corresponding author: Phone: +34 935 94 77 00 - 2201

xavier.munoz@imb-cnm-csic.es

## Abstract

At the point of care (POC), on-side clinical testing allows fast biomarkers determination even in resource-limited environments. Current POC systems rely on tests selective to a single analyte or complex multiplexed systems with important portability and performance limitations. Hence, there is a need for handheld POC devices enabling the detection of multiple analytes with accuracy and simplicity. Here we present a reconfigurable smartphone-interfaced electrochemical Lab-on-a-Chip (LoC) with two working electrodes for dual analyte determination enabling biomarkers' selection in situ and on-demand. Biomarkers selection was achieved by the use of electrodeposable alginate hydrogels. Alginate membranes containing either glucose oxidase (GOx) or lactate oxidase (LOx) were selectively electrodeposited on the surface of each working electrode in around 4 min, completing sample measurement in less than 1 min. Glucose and lactate determination was performed simultaneously and without cross-talk in buffer, fetal bovine serum (FBS) and whole blood samples, the latter being possible by the size-exclusion filtration capacity of the hydrogels. At optimal conditions, glucose and lactate were determined in a wide linear range (0 -12 mM and 0 – 5 mM, respectively) and with high sensitivities (0.24 and 0.54  $\mu\text{A cm}^{-2} \text{mM}^{-1}$ , respectively), which allowed monitoring of Type-1 diabetic patients with a simple dual analysis system. After the measurement, membranes were removed by disaggregation with the calcium-chelator phosphate buffer. At this point, new membranes could be electrodeposited, this time being selective to the same or another analyte. This conferred the system with on-demand biomarkers' selection capacity. The versatility and flexibility of the current architecture is expected to impact in POC analysis in applications ranging from homecare to sanitary emergencies.

## 1. Introduction

Point of care (POC) systems have impacted in clinical diagnosis for enabling diagnostic tests out of central medical laboratories and near the side of patient care.(Gubala et al., 2012)·(Hu et al., 2014)·(Gervais et al., 2011) Their advantages include low-cost, simplicity, portability, miniaturization and minimal user intervention, which make them ideal to operate in resources-limited environments such as developing countries, the bedside of the patient or at home.(Nayak et al., 2017) From the 80s, many POC tests for fast and accurate on-side determination of glucose,(Yoo and Lee, 2010) lipids,(Lu et al., 2017) glycohemoglobin (HbA1c),(Hirst et al., 2017) hepatitis C virus (HCV),(Khuroo et al., 2015) immunodeficiency virus (HIV),(Shafiee et al., 2015) influenza,(Tuttle et al., 2015) urinalysis,(Lin et al., 2011) hematology,(Sireci, 2015) several types of cancer,(Lewis et al., 2015)·(Shadfan et al., 2015)·(Mohammed et al., 2016)·(Lewis et al., 2015) pregnancy(Majors et al., 2017) or prothrombin(Perry et al., 2010) have been produced and commercialized, mostly based on lateral flow test or immunoassays.(Mahato et al., 2018)·(Mahato et al., 2017)

Main limitations of current POC systems rely on the poor versatility and adaptability of the tests. That is, most POC systems are restricted to a single analyte and the application to another one requires the almost complete redesign of the test and/or the device. This is quite limiting since, in many cases, an appropriate diagnosis or treatment monitoring requires clinical evidences from more than one analyte.(Berhane et al., 2014) This is the case of type 1 diabetes mellitus, a global life-threatening pathology with an incidence rate per annum of 3.4%.(Patterson et al., 2018) Analysis of early metabolic changes during the development and progression of diabetes is crucial to the management of the disease. Among these changes, determination of circulating lactate, in addition to glycaemia, has been reported to be a helpful predictor of poorly regulated type 1

diabetes mellitus.(Brouwers et al., 2015) In addition, recent reports on antidiabetic drugs have revealed novel mechanisms of action involving substantial changes on lactate and related metabolites.(Alfaras et al., 2017; Silva et al., 2010) Therefore, monitoring both glucose and lactate lead, not only for an early detection of diabetes, but also shed light on novel targets and signalling pathways regulating the disease.

Multiplexed systems may solve this problem by providing a way to determine multiple analytes from a single specimen.(Dincer et al., 2017)(Díaz-González et al., 2014) Currently, they consist of combinations of individual tests spatially or regionally separated from the others by spots,(Lee et al., 2015) wells,(Shen et al., 2010) independent channels (channel networks)(Tian et al., 2016) or electrodes (electrode arrays).(Wang et al., 2015) Each spot, well, channel or electrode is functionalized to recognize one analyte and this selectivity cannot be modified over time. Since each detection area/element is operated individually, multiplexed systems normally require complex and bulky instruments difficult to operate out of the laboratory. The few portable multiplexed systems, also known as multiplexed POC,(Díaz-González et al., 2014) are mostly single use and present limited multiplexing capacities and poor versatility.

In an attempt to solve this open issue, a cost-effective, miniaturized, portable and smartphone-interfaced POC system has been developed, which provides multi-analyte determination in whole blood and in situ selection of the analyte on-demand. Analyte selection is achieved by means of electro-addressable and selective alginate hydrogel membranes. Alginate electrodeposition is achieved by acidic dissociation of calcium carbonate particles.(Cheng et al., 2011) That is, water splitting produces the local acidification of the medium and calcium release in the vicinity of the working electrode. This process leads to the formation of alginate hydrogels on the working electrode, with spatial resolution and thickness control.(Márquez et al., 2017) The presence of selective recognition biomolecules,

e.g. enzymes, in the alginate precursor solution enables the generation of selective bio-recognition membranes in situ (Márquez et al., 2017) (Márquez-Maqueda et al., 2016) and the selection of the analyte on-demand. Alginate membranes present additional advantages such as long-term stability of the biomolecules and filtering capacity, enabling the measurement in whole blood samples without additional separation steps. (Márquez et al., 2017) These membranes, moreover, disaggregate at room temperature when immersed in a solution containing a calcium chelator solution, e.g. phosphate buffer. After that, the membrane can be re-generated and the removal/re-generation process can be repeated multiple times. This confers the Lab-on-a-Chip (LoC) with high versatility and adaptability, since the re-generated membrane can contain the same or another biorecognition element, enabling the determination of multiple analytes with the same simple and miniaturized system.

This smartphone-based POC present, therefore, (i) high-versatility, adaptability and capacity for whole blood analysis by the use of electrodepositable alginate hydrogels as selective membranes; (ii) durability, sensitivity and accuracy in the measurement by incorporating silicon-based micro-electrodes obtained by microfabrication technologies; and (iii) simplicity, portability and lightweight by combining a simple microfluidic architecture on poly(methyl) methacrylate (PMMA) and polydimethylsiloxane (PDMS) with a minimalistic  $\mu$ -Potentiostat controlled and powered by the smartphone (without the need of external batteries). The performance of the reconfigurable multiplexed POC system is here evaluated in the identification of Type-I diabetic patients through the measurement of glucose and lactate.

## **2. Materials and Methods**

### **2.1. Reagents**

Alginic acid sodium salt,  $\text{CaCl}_2$  ( $\geq 93$  %), 2-(N-morpholino)ethanesulfonic acid hydrate (MES hydrate,  $\geq 99$  %),  $\text{NaOH}$  ( $\geq 98$  %),  $\text{KOH}$  ( $\geq 86$  %), 3,3',5,5'-Tetramethylbenzidine dihydrochloride hydrate (TMB,  $\geq 98$  %),  $\text{NaCl}$  (ACS reagent,  $\geq 99$  %),  $\text{H}_2\text{O}_2$  (30% in  $\text{H}_2\text{O}$ ),  $\text{AgNO}_3$  ( $\geq 99$  %),  $\text{K}_4[\text{Fe}(\text{CN})_6]$  (ACS Reagent,  $\geq 98.5$  %), D-(+)-Glucose ( $\geq 99.5$  %), sodium L-lactate ( $\sim 98$  %),  $\text{HNO}_3$  ( $\geq 69$  %), peroxidase (HRP; Type VI-A, essentially salt-free lyophilized powder, 250-330 units  $\text{mg}^{-1}$ ), glucose oxidase (GOx) from *Aspergillus niger* (Type X-S, lyophilized powder, 100–250 units  $\text{mg}^{-1}$ ) and lactate oxidase (LOx) from *Pediococcus sp.* (lyophilized powder,  $\geq 20$  units  $\text{mg}^{-1}$ ) were purchased from Sigma-Aldrich.  $\text{CaCO}_3$  ( $\geq 98.5$  %),  $\text{K}_3[\text{Fe}(\text{CN})_6]$  (ACS reagent,  $\geq 99$  %),  $\text{Na}_2\text{HPO}_4$  (ACS reagent,  $\geq 99$  %), ethanol absolute ( $\geq 99.5$  %),  $\text{H}_2\text{SO}_4$  (96 %) and  $\text{HCl}$  (37%) were purchased from Panreac.  $\text{KCl}$  ( $\geq 99$  %),  $\text{KH}_2\text{PO}_4$  (ACS reagent,  $\geq 99.5$  %) and L-(+)-tartaric acid ( $\geq 99$  %) were purchased from Fluka. Polydimethylsiloxane (PDMS) was purchased from Sylgard and casted and polymerized by heating at 80 °C in 1 mm thick layers previous mechanization by laser ablation. Fetal bovine serum (FBS) was provided by Capricorn Scientific (Ebsdorfergrund, Germany).

All chemicals were used as received and aqueous solutions were prepared using de-ionized water with a resistivity of 2 M  $\Omega$  cm. Used PBS contains  $\text{NaCl}$  (8 g  $\text{L}^{-1}$ ),  $\text{KCl}$  (0.2 g  $\text{L}^{-1}$ ),  $\text{Na}_2\text{HPO}_4$  (1.42 g  $\text{L}^{-1}$ ) and  $\text{KH}_2\text{PO}_4$  (0.24 g  $\text{L}^{-1}$ ). TMB 25 mM stock aqueous solution was daily prepared. Whole blood was extracted from a volunteer and stored at 4° C until measurement.

Polymethylmethacrylate (PMMA) foils of different thicknesses (0.5, 1 and 2 mm) were purchased from Goodfellow and clear polyester double-sided adhesive tape from ARcare. The adhesive is MA-93 acrylic medical grade, also known as pressure sensitive adhesive (PSA).

## 2.2. Equipment

Electrochemical measurements were done using Autolab electrochemical workstation (PGSTAT-100 potentiostat - galvanostat, Ecochemie, Utrecht, The Netherlands) controlled using a PC with NOVA software for comparison with the developed  $\mu$ Potentiostat. The reliability of the pseudo-reference was checked using external reference (Orion 92-02-00, Thermo Fisher Scientific Inc., Beverly USA).

Electrodepositions of Ag and chlorination were performed using a Keithley 2430 1 kW pulse Source Measure Unit and a Watson Marlow peristaltic pump to maintain a constant flow of the reactants.

PMMA and PDMS mechanization was done using an Epilog Mini 24 Laser. For the designs, Corel Draw X7 software was used.

### **2.3. Design of the POC system**

The smartphone-based POC was designed and fabricated differentiating three main parts (**Figure 1**), namely i) the silicon chip for amperometric measurements, ii) the microfluidic structure for fluid management and chip packaging, and iii) the smartphone-interfaced  $\mu$ Potentiostat, designed and manufactured with discrete elements to control measurement. Each component is described in separate in the following sections.

#### **Silicon chip**

Silicon chips manufactured by high-precision microfabrication technologies were selected as electrochemical transducers for being highly repetitive, stable and durable enabling multiple measurements without losing activity. The design of the chip included four rectangular platinum electrodes corresponding to the working (WE; two working electrodes), reference (RE) and counter electrodes (CE), this last one with a larger area to avoid charge transfer limitations. The electrodes in

the chip were connected to independent pads of big size to facilitate the external connection to the potentiostat through spring-loaded connectors.

The four electrode silicon chips were fabricated in a well established lift-off process in the Clean Room facilities of the IMB-CNM, by a protocol previously described by our group.(Orozco et al., 2007) Briefly, a silicon wafer was exposed to thermal oxidation to obtain a first SiO<sub>2</sub> layer of 1000 nm. Afterwards, a photoresist was spread over the oxidized wafer by spin coating and cured by UV irradiation developing only the SiO<sub>2</sub> areas for metal covering. Two metal layers were subsequently deposited, namely a 20 nm layer of Cr to enhance the adhesion of Pt, and the Pt layer of 100 nm. The photoresist was then removed by immersion in acetone and therefore also the metal over it, while the metal directly deposited on the wafer remained, comprising the electrodes, connections and pads.

A subsequent step for electrodes protection was performed consisting of a first SiO<sub>2</sub> deposition by Plasma Enhanced Chemical Vapour Deposition, which covered the electrodes. After that, a layer of photoresist was spread, cured and developed, allowing the wet etching of an area over the metal using buffered hydrofluoric acid solution. These steps avoided the direct exposure to the solution of the edges of the electrodes, increasing their robustness and durability. In the end, the excess of photoresist was removed with acetone.

The reference electrode was modified with an already reported electrodeposition/chlorination protocol(Zarkadas et al., 2001) to produce a Ag/AgCl pseudo reference electrode. Before Ag electrodeposition, the electrode was cleaned with 96 % ethanol, 6 M H<sub>2</sub>SO<sub>4</sub> and finally immersed in 50 mM KOH and 25 % H<sub>2</sub>O<sub>2</sub> solution for 15 min to eliminate any contamination of the surface. The silicon chip was then introduced in an electrodeposition chamber (**Figure S1**) containing a second silicon chip in front of the previous one and separated at a distance of 1 mm to make the electrodeposition process more homogeneous. The electrodeposition of the Ag layer was done galvanostatically while a constant flow



of tartaric acid and  $\text{AgNO}_3$  solution was passed through the chamber. After Ag deposition the Ag layer was partially chloritized, also galvanostatically, with a solution of KCl and HCl passing through the chamber. Obtained reference potential was comparable to those supplied by commercial reference electrodes. The potential shift between the commercial and the fabricated Ag/AgCl electrode was only of 25 mV while the shift, in case of using the bare Pt electrode as reference, was situated at 180 mV (**Figure S2**).

The integrated pseudo-reference electrode demonstrated long-term stability and durability, supplying the same potential over time at least for 2 months, values that were completely comparable to the commercial one.

### **Microfluidic architecture**

The microfluidic architecture was fabricated in PMMA/PDMS by  $\text{CO}_2$  laser ablation. The patterning of PMMA foils was used to construct, layer by layer, a device with the silicon chip footprint and microfluidic channels and connections for (i) fluid management, (ii) stable and robust electrode packaging and (iii) the isolation of the pad connectors.

The construction of the microfluidic structure resulted from the assembling of three parts, namely a) the base, c) the microfluidic part and e) the cover (**Figure 1**, left). Each one of these parts was composed of two or more PMMA layers bonded through PSA. A detailed description of the construction of the device is depicted in **Figure S3**. Briefly, the base contained two PMMA layers, a 0.5 mm PMMA layer patterned with the chip footprint to stably immobilize the silicon piece, and a 2 mm layer used as support. Over the base, the microfluidic part contained all the microfluidic elements for liquid management. This part was composed of three PMMA layers: the intermediate layer (1 mm thick) comprising the channels and the measurement chamber, and two adjacent layers (0.5 mm thick each) sealing the channels but not the measurement chamber. Finally, the cover was positioned

over the microfluidic part to seal the system. This part included a movable PMMA element with a small aperture for opening-closing the access to the measurement chamber. This element enabled a dual filling mechanism of the measurement chamber. On the one hand, when closed, the measurement chamber could be filled through the fluidic inlet without leakage (**Figure S4**). When opened, it allowed the introduction of small sample volumes directly to the measurement chamber and the transducers, avoiding dead volumes and enabling to work with small sample volumes. This second operation mechanism was of particular interest in the case of blood samples, where, for practical applications, the sample volume was restricted to a blood drop of few  $\mu\text{L}$ .

The three parts were finally assembled using screws and PDMS layers as junctions to avoid fluid leakage. Two fluidic connections were introduced and bonded to the fluidic channels corresponding to the fluidic inlet and outlet of the device. The fluidic connections were sealed with epoxy resist.

### **Smartphone-interfaced $\mu$ Potentiostat**

The custom made potentiostat resembled our previous publication (Aymerich et al., 2018). It was designed to execute the following basic functions: (i) to operate the sensor in potentiostatic mode, (ii) to read the transduced signal, (iii) to convert it into the digital domain and (iv) to provide the data link through USB on-the-go protocol. In this way, bidirectional data transmission and powering of the system was provided avoiding the use of batteries. All these functions were implemented adding few discrete electrical components to the LoC, and ensuring the low cost, small size, simplicity and lightweight of the POC system (**Figure 1**, right). The minimalistic electronic design only required one standard microcontroller (ATMega32U4), two operational amplifiers (AD4692), resistors and capacitors. The combination of all these components implemented an analog-to-digital delta-sigma converter with tuneable read-out range between 1nA to 100 $\mu\text{A}$ . The

potentiostatic system enabled two operation modes, namely chronoamperometry, used for analyte detection, and cyclic voltammetry, this required for membrane electrodeposition. In both cases, the potential voltage was programmed between +/- 1.65 V. In the cyclic voltammetry mode, the scan rate was adjusted between 2 to 200mV/s.

#### **2.4. In situ production and re-generation of alginate membranes**

The element conferring selectivity, versatility and reversibility to the smartphone-interfaced POC system was the electrodeposable alginate hydrogel used as biocatalytic membrane by incorporation of enzymes. The in situ generation and removal of the alginate membrane was based on an already reported protocol (Cheng et al., 2011) adapted to the LoC architecture. First, the hydrogel precursor solution was injected into the device through the lateral fluidic connections. The precursor solution contained the enzymes, 1 % w/v sodium alginate and 0.5 % w/v CaCO<sub>3</sub>. A potential of +1.4 V (vs. Ag/AgCl) was then applied to the WE for 90 s promoting water splitting into O<sub>2</sub> and protons. The produced protons locally acidified the WE vicinity, dissolving CaCO<sub>3</sub> particles and releasing Ca<sup>2+</sup> cations. These Ca<sup>2+</sup> cations induced alginate jellification by cross-linking of alginate monomers, resulting in a high hydrated gel over the WE. Due to the hydrogel porosity, enzymes were stably entrapped in the alginate matrix. The non-polymerized precursor solution was collected for further electrodepositions and the membrane was rinsed with distilled water to eliminate the excess of precursor. The electrodeposition process could be then repeated in the second WE with a precursor solution selective to another analyte.

After measurement, the biocatalytic membranes were removed by disaggregation with the Ca<sup>2+</sup> cation chelating agent phosphate buffer. A constant flow of phosphate buffer through the lateral connections was used to remove the membrane from the WEs surface. Alginate hydrogel removal enabled the recovering of the transducer, which could

be re-used after biofunctionalization with biocatalytic membranes of the same composition or another selectivity of interest. Thus, multiple biomarkers detection and on-demand selection of the analyte could be achieved combining the two available working electrodes. The formation/removal processes are illustrated in **Figure 2**, **Figure S5 (for removal)** and the **video** included in the Supplementary Information.

## 2.5. Glucose and lactate determination

The detection of glucose and lactate was done indirectly in an oxidase-peroxidase enzymatic cascade using TMB as redox mediator. In the detection, the analyte was firstly oxidized by the specific oxidase enzyme, either glucose oxidase in the case of glucose or lactate oxidase for lactate. In both cases, the oxidation of the biomarker produced  $H_2O_2$ , which was subsequently reduced to water by the peroxidase, i.e. HRP, the latter producing the oxidation of the TMB. Applying a reduction potential of 0.1 V vs pseudo Ag/AgCl, the enzymatically oxidized TMB was determined, with a current magnitude directly proportional to the analyte concentration.

In the calibration, a constant current was recorded while the buffer was flowing through the chamber without analyte. Then, when a known concentration of the analyte of interest was added into the measurement chamber, a fall in the current was registered (**Figure S6**).

In the case of FBS, whole blood analysis and real samples, the open-close access to the measurement chamber was used in order to minimize the sample volume. With the current design, the system required a volume between 30 and 50  $\mu$ L per assay. In the calibration with FBS and whole blood, the samples were spiked with glucose and lactate to adapt the final concentration to the ranges of interest. In the case of real samples from diabetic and control mice, plasma was obtained after blood centrifugation (10000 g, 5 min, room temperature). Glucose and lactate concentrations in these real samples were measured in the POC system and the

results were compared to those determined at the Servei de Bioquímica Clínica Veterinària of the Universitat Autònoma de Barcelona with an Automated Clinical Chemistry Analyzer (Olympus AU480) by enzymatic-based assays.

## **2.6. Diabetes induction and blood samples processing**

C57BL/6 male mice (8-10 weeks) were randomly assigned to the control (vehicle) (n=6) or diabetic group (n=6). Mice were housed in a temperature- and light-controlled room with free access to water and normal chow diet. Diabetes was induced in fasted mice by intraperitoneal injection of streptozotocin (STZ) (50 mg/kg/day) (Sigma-Aldrich, Madrid, Spain) for 5 consecutive days, whereas animals in the control group received vehicle (0.1 M sodium citrate buffer, pH 4.5). After 21 days, the presence of diabetes was established by the presence of plasma glucose levels higher than 250 mg/dl. Mice were sacrificed 8 weeks later and the blood was used for plasmatic determination of glucose and lactate by specific enzymatic-based assays following manufacturer's instructions. All animal procedures were performed in agreement with the European guidelines (2010/63/EU) and approved by the University of Barcelona Local Ethical Committee.

## **3. Results and Discussion**

### **3.1. In situ generation and removal of the biocatalytic membranes in the POC system**

The performance of the smartphone-interfaced POC system was analysed in the laboratory for the determination of glucose and lactate in MES buffered solutions. The protocol to demonstrate the versatility and adaptability of the POC system is illustrated in **Figure 2**. First, the empty chamber containing the four electrodes for amperometric measurements (**Figure 2a**) was filled with the alginate hydrogel

precursor solution containing GOx and HRP (**Figure 2b**). After applying an electrodeposition potential of 1.4 V vs. Ag/AgCl pseudo-reference for 90 s (**Figure 2c**) and rinsing with distilled water to remove the excess material a biocatalytic membrane selective to glucose was generated on the first WE surface (**Figure 2d**). In a similar process (**Figure 2e, 2f**), a membrane selective to lactate was electrodeposited over the second WE, by the substitution of GOx by LOx in the second injected precursor.

At this point, the introduction of a glucose containing solution first (**Figure 2g**) and a lactate containing solution afterwards (**Figure 2h**), produced the selective oxidation of the analyte and hence the mediator (TMB), which changed from uncoloured to blue as can be appreciated in the respective membranes.

The oxidized TMB concentration, proportional to the analytes, was determined amperometrically at 0.1 V vs pseudo Ag/AgCl, the reduction potential of the TMB. The biocatalytic membranes were then removed by injection of a phosphate buffered solution (**Figure 2i**), and could be re-generated afterwards following the same protocol and enabling in situ selection of biomarkers on demand.

### **3.2. Simultaneous determination of multiple analytes and cross-talk analysis in serum samples**

In the sequential determination of multiple analytes with the smartphone-interfaced POC system, glucose and lactate were selected as biomarkers for their interest in identification and monitoring of type 1 diabetes patients. In both cases, the biosensor response was maximized in separate prior to the calibration in FBS to guarantee optimal measurement conditions. By adjusting the concentration of enzyme in the biocatalytic membrane, it was possible to adapt the linear response of the biosensor to the analyte level in real samples. Concretely, HRP content in the precursor solution was fixed to 15 activity units mL<sup>-1</sup> and the content of GOx

and LOx was increased until reaching maximum amperometric response for the largest analyte concentration of interest (Márquez et al., 2017), i.e. 10 mM glucose and 5 mM lactate in case of human samples and 70 mM glucose and 10 mM lactate in case of mice. According to this, the optimal GOx and LOx concentrations were set at 2 and 10 activity units ml<sup>-1</sup> and 0.2 and 5 activity units ml<sup>-1</sup>, respectively. The results for the two optimizations were in agreement with the maximum current density allowed by the amperometric system since in both cases reached a value close to 4 μA cm<sup>-2</sup>.

Under optimal condition, the glucose biosensor presented a sensitivity (S) of 0.33 μA cm<sup>-2</sup> mM<sup>-1</sup> and a limit of detection (LOD) of 0.18 mM while the lactate biosensor has a S of 0.78 μA cm<sup>-2</sup> mM<sup>-1</sup> and a LOD of 0.12 mM. LOD was determined considering the 3 sigma method (three times the standard deviation of the blank). After biosensor optimization, several detection cycles combining glucose and lactate determinations were carried out to validate the biosensors and to obtain the calibration curves for glucose and lactate in FBS (**Figure 3**). Detection cycles comprised i) biocatalytic membranes generation, ii) rinsing, iii) simultaneous detection of the analytes and iv) membrane removal with phosphate buffer, as detailed previously. In each cycle, a single analyte concentration was determined for glucose and lactate. The replicas for a single biomarker concentration were therefore obtained from five independent membranes subsequently formed and removed. In the glucose determination (**Figure 3a**), good repeatability in the generated membranes was observed in the whole linear range with variation coefficients below 10 % in all cases. The calibration curve also presented good responses with a linear range from 0 to 10 mM ( $R^2 = 0.99$ ) that ensured an accurate determination of the analyte in the range of interest. Due to the high repeatability of the membranes and the durability and stability of the micro-fabricated electrodes, it was not necessary to recalibrate the system between measurements, simplifying the assay and improving the performance of the whole

POC system. Similarly, lactate determination provided repetitive values from individually generated and removed membranes (**Figure 3b**), with good repeatability and variation coefficients of 25 % for low concentrations (< 2 mM) but below 10% for concentrations over 2 mM, as well as a good calibration curve with large linear range from 0 to 2 mM ( $R^2 = 0.99$ ).

When the electrodeposited membranes lacked of the necessary enzymes for the detection of one of the analytes (**Figure 3c**), the amperometric system lost the capacity to respond to that, regardless the concentration of analyte in the sample. In addition, when both enzymes are present in the respective hydrogel, two signals were obtained, being proportional to the glucose and lactate concentrations and absolutely comparable to the previous results from individual calibrations. Thus, the measurement of glucose did not interfere lactate determination, and vice versa. This fact demonstrated that it was not cross talk between consecutively generated membranes or among the two working electrodes during the same measurement.

### **3.3. Whole blood sample analysis**

In the case of blood, samples were introduced to the POC system through the aperture present in the top piece of the microfluidic architecture to minimize sample consumption and dead volumes. The top aperture was closed during the precursor injection, electrodeposition, precursor recovery and chamber rinsing (**Figure 4a**). The pressure provided by the screws together with the PDMS layers avoided any leakage from the chamber during all these processes. The aperture was opened for whole blood analysis, which enable the introduction of the sample directly on top of the biosensor (**Figure 4b**). Once the signal was recorded, the gate was closed again and the chamber was washed with PBS first and finally with water for sample and membrane removal.



The alginate membrane was demonstrated to act not only as retention matrix for enzymes immobilization but also as a size-exclusion filter, enabling the retention of the cell fraction of the blood and minimizing biofouling (Márquez et al., 2017). This is of particular interest in the analysis of complex samples, e.g. whole blood. This capacity was employed in the present work in the determination of glucose and lactate in whole blood samples without additional separation or purification steps.

Blood samples were spiked with glucose doses emulating real situations of healthy persons, pre-diabetic and diabetic patients. When compared to analyte detection in buffer solutions, the sensitivity of both glucose and lactate decreased significantly with whole blood (**Figure 4c, 4d**). Concretely, it was reduced a 27 % (S in whole blood = 0.24  $\mu\text{A cm}^{-2} \text{mM}^{-1}$ ) for glucose and a 31% (S in whole blood = 0.54  $\mu\text{A cm}^{-2} \text{mM}^{-1}$ ) for lactate, mostly attributed to matrix effects. On the contrary, the LODs did not change in any case.

In terms of linear range, the biosensors presented larger linear ranges for glucose (from 0 to 12 mM) and lactate (from 0 to 5 mM), which allowed to distinguish between healthy and unhealthy levels of analyte. That is, glucose levels between 4 and 5 mM were considered normal, from 6 to 8 mM risky and over 8 mM were clearly related to diabetic condition. Similarly, lactate levels may be indicative of many pathological states. For example, below 1 mM may be normal and over 2 mM were related to sepsis. (Lee and An, 2016) Regarding diabetic patients, which was the case of study, lactate concentration between 5 and 7 mM were considered normal and below 4 mM pathological or indicative of type 1 diabetes.

Finally, the system maintained the high repeatability of the biocatalytic membranes, with variation coefficients below 20 %, which allowed analyte determination without constant recalibration of the system.

In conclusion, the current smartphone-interfaced POC system enabled on-demand selection of target molecules and multiple analyte determination in whole blood samples by in situ production/removal of biocatalytic membranes based on alginate hydrogels.

### **3.4. Real sample analysis and type 1 diabetes diagnosis**

STZ-induced diabetic mice displayed fasting plasma glucose levels 5 times higher than the control group (Figure 5a) with a substantial reduction in plasma lactate concentrations (Figure 5c) with both methods. Results from the reconfigurable multiplexed POC system were in perfect agreement with the standard method. This was clear when evaluating the quantile-quantile (Q-Q) plots presented in Figure 5b and 5d and corresponding to the comparison of the standard method with the POC system in the determination of glucose and lactate, respectively. As show, both plots presented good linearity ( $R^2=0.99$ ) and comparable results, with a slope magnitude of 1 and y-intercept of 0.

Regarding the clinical relevance of the results, these data were in line with a previous report in which STZ-induced diabetic mice showed hyperglycaemia with a concomitant falling in circulating lactate levels.(Silva et al., 2010) Interestingly, treatment of these mice with metformin reduced glycemia and restored lactate levels via direct stimulation of major glycolytic enzymes.(Silva et al., 2010) The authors of this study concluded that activation of glycolysis contributes to the hypoglycemic effect of this drug. These findings might imply that type 1 diabetic patients with low lactate levels would benefit from the treatment with drugs, such as metformin, that stimulate glycolysis. In agreement with this, it has been recently reported that metformin improves insulin sensitivity in youth with type 1 diabetes mellitus.(Bjornstad et al., 2018) It would be interesting to study whether the improvement in the control of the disease in type 1 diabetic patients correlates with the restoration of lactate levels following metformin treatment.

## **4. Conclusions**

A reconfigurable multiplexed POC system enabling in situ selection and electrochemical determination of multiple analytes in blood samples is developed and applied to the identification of type 1 diabetic patients. The POC system combines three main components: i) a micro-fabricated silicon chip that guarantees reproducibility, accuracy, durability and robustness; ii) a costless polymer-based microfluidic structure enabling electrodes packaging and fluid management in two microfluidic configurations, i.e. lateral fluidic connections for membranes generation/removal and chip washing and a top aperture for low volume sample introduction; and iii) a dedicated and reconfigurable  $\mu$ potentiostat, controlled and powered by the smartphone, which enables cyclic voltammetries and chronoamperometric measurements with the capacity of detecting currents in the range of nA. The use of electrodepositable alginate hydrogels as biocatalytic membranes confer the system with additional features, i.e. flexibility – membranes are generated in situ and removed after measurement enabling analyte selection on demand-, capacity to measure in whole blood samples –by the size-exclusion capacity of the gels-. Glucose and lactate are determined in buffer, serum and whole blood samples without cross-talk and in the adequate range for human disease control and prevention (e.g. diabetes and sepsis). The high portability of the complete system, together with the analytical versatility of the alginate membranes and the reusability of the electrodes due to the membrane protection qualifies this prototype to be used in healthcare centres and at home, but also in resource-limited environments such as in any location where a health emergency is taking place.

### **Acknowledgements**

This work was supported by the Spanish R & D National Program (MEC Project TEC2014-54449-C3-1-R). Dr. X. M.-B. also acknowledge the “Ramón y Cajal” program from the Spanish Government. A.M. is also grateful to the MICINN for the award of a research studentship from FPI program (BES-2015-072946).

## Notes and references

- Alfaras, I., Mitchell, S.J., Mora, H., Lugo, D.R., Warren, A., Navas-Enamorado, I., Hoffmann, V., Hine, C., Mitchell, J.R., Le Couteur, D.G., Cogger, V.C., Bernier, M., de Cabo, R., 2017. Health benefits of late-onset metformin treatment every other week in mice. *NPJ aging Mech. Dis.* 3, 16. doi:10.1038/s41514-017-0018-7
- Aymerich, J., Márquez, A., Terés, L., Muñoz-Berbel, X., Jiménez, C., Domínguez, C., Serra-Graells, F., Dei, M., 2018. Cost-effective smartphone-based reconfigurable electrochemical instrument for alcohol determination in whole blood samples. *Biosens. Bioelectron.* 117, 736–742. doi:10.1016/j.bios.2018.06.044
- Berhane, F., Fite, a., Daboul, N., Al-Janabi, W., Msallaty, Z., Caruso, M., Lewis, M.K., Yi, Z., Diamond, M.P., Abou-Samra, a. B., Seyoum, B., 2014. I.27 Plasma lactate levels increase during hyperinsulinemic euglycemic clamp and oral glucose tolerance test. *Diabetes Res. Clin. Pract.* 103, S8. doi:10.1016/S0168-8227(14)70028-2
- Bjornstad, P., Schäfer, M., Truong, U., Cree-Green, M., Pyle, L., Baumgartner, A., Garcia Reyes, Y., Maniatis, A., Nayak, S., Wadwa, R.P., Browne, L.P., Reusch, J.E.B., Nadeau, K.J., 2018. Metformin Improves Insulin Sensitivity and Vascular Health in Youth With Type 1 Diabetes Mellitus. *Circulation* 138, 2895–2907. doi:10.1161/CIRCULATIONAHA.118.035525
- Brouwers, M.C.G.J., Ham, J.C., Wisse, E., Misra, S., Landewe, S., Rosenthal, M., Patel, D., Oliver, N., Bilo, H.J.G., Murphy, E., 2015. Elevated lactate levels in patients with poorly regulated type 1 diabetes and glycogenic hepatopathy: a new feature of Mauriac syndrome. *Diabetes Care* 38, e11-2. doi:10.2337/dc14-2205
- Cheng, Y., Luo, X., Betz, J., Payne, G.F., Bentley, W.E., Rubloff, G.W., 2011. Mechanism of anodic electrodeposition of calcium alginate. *Soft Matter* 7, 5677. doi:10.1039/c1sm05210a
- Díaz-González, M., Muñoz-Berbel, X., Jiménez-Jorquera, C., Baldi, A., Fernández-Sánchez, C., 2014. Diagnostics Using Multiplexed Electrochemical Readout

- Devices. *Electroanalysis* 26, 1154–1170. doi:10.1002/elan.201400015
- Dincer, C., Bruch, R., Kling, A., Dittrich, P.S., Urban, G.A., 2017. Multiplexed Point-of-Care Testing – xPOCT. *Trends Biotechnol.* 35, 728–742.  
doi:10.1016/j.tibtech.2017.03.013
- Gervais, L., De Rooij, N., Delamarche, E., 2011. Microfluidic chips for point-of-care immunodiagnosics. *Adv. Mater.* 23. doi:10.1002/adma.201100464
- Gubala, V., Harris, L.F., Ricco, A.J., Tan, M.X., Williams, D.E., 2012. Point of care diagnostics: Status and future. *Anal. Chem.* 84, 487–515. doi:10.1021/ac2030199
- Hirst, J.A., McLellan, J.H., Price, C.P., English, E., Feakins, B.G., Stevens, R.J., Farmer, A.J., 2017. Performance of point-of-care HbA1c test devices: Implications for use in clinical practice - A systematic review and meta-analysis. *Clin. Chem. Lab. Med.* 55, 167–180. doi:10.1515/cclm-2016-0303
- Hu, J., Wang, S.Q., Wang, L., Li, F., Pingguan-Murphy, B., Lu, T.J., Xu, F., 2014. Advances in paper-based point-of-care diagnostics. *Biosens. Bioelectron.* 54, 585–597. doi:10.1016/j.bios.2013.10.075
- Khuroo, M.S., Khuroo, N.S., Khuroo, M.S., 2015. Diagnostic accuracy of point-of-care tests for hepatitis C virus infection: A systematic review and meta-analysis. *PLoS One* 10, 1–22. doi:10.1371/journal.pone.0121450
- Lee, J.H., Seo, H.S., Kwon, J.H., Kim, H.T., Kwon, K.C., Sim, S.J., Cha, Y.J., Lee, J., 2015. Multiplex diagnosis of viral infectious diseases (AIDS, hepatitis C, and hepatitis A) based on point of care lateral flow assay using engineered proteinticles. *Biosens. Bioelectron.* 69, 213–225. doi:10.1016/j.bios.2015.02.033
- Lee, S.M., An, W.S., 2016. New clinical criteria for septic shock: serum lactate level as new emerging vital sign. *J. Thorac. Dis.* 8, 1388–1390.  
doi:10.21037/jtd.2016.05.55
- Lewis, J.M., Heineck, D.P., Heller, M.J., 2015. Detecting cancer biomarkers in blood: Challenges for new molecular diagnostic and point-of-care tests using cell-free nucleic acids. *Expert Rev. Mol. Diagn.* 15, 1187–1200.

doi:10.1586/14737159.2015.1069709

- Lin, C.-C., Tseng, C.-C., Chuang, T.-K., Lee, D.-S., Lee, G.-B., 2011. Urine analysis in microfluidic devices. *Analyst* 136, 2669. doi:10.1039/c1an15029d
- Lu, S., Yu, T., Wang, Y., Liang, L.-G., Chen, Y., Xu, F., Wang, S., 2017. Nanomaterial-based Biosensors for Measurement of Lipids and Lipoproteins towards Point-of-Care of Cardiovascular Disease. *Analyst* 3309–3321. doi:10.1039/C7AN00847C
- Mahato, K., Maurya, P.K., Chandra, P., 2018. Fundamentals and commercial aspects of nanobiosensors in point-of-care clinical diagnostics. *3 Biotech* 8, 1–14. doi:10.1007/s13205-018-1148-8
- Mahato, K., Srivastava, A., Chandra, P., 2017. Paper based diagnostics for personalized health care: Emerging technologies and commercial aspects. *Biosens. Bioelectron.* 96, 246–259. doi:10.1016/j.bios.2017.05.001
- Majors, C.E., Smith, C.A., Natoli, M.E., Kundrod, K.A., Richards-Kortum, R., 2017. Point-of-care diagnostics to improve maternal and neonatal health in low-resource settings. *Lab Chip* 17, 3351–3387. doi:10.1039/C7LC00374A
- Márquez-Maqueda, A., Ríos-Gallardo, J.M., Vigués, N., Pujol, F., Díaz-González, M., Mas, J., Jiménez-Jorquera, C., Domínguez, C., Muñoz-Berbel, X., 2016. Enzymatic Biosensors Based on Electrodeposited Alginate Hydrogels. *Procedia Eng.* 168, 622–625. doi:10.1016/j.proeng.2016.11.229
- Márquez, A., Jiménez-Jorquera, C., Domínguez, C., Muñoz-Berbel, X., 2017. Electrodepositable alginate membranes for enzymatic sensors: An amperometric glucose biosensor for whole blood analysis. *Biosens. Bioelectron.* 97, 136–142. doi:10.1016/j.bios.2017.05.051
- Mohammed, S.I., Ren, W., Flowers, L., Rajwa, B., Chibwasha, C.J., Parham, G.P., Irudayaraj, J.M.K., 2016. Point-of-care test for cervical cancer in LMICs. *Oncotarget* 7, 18787–18797. doi:10.18632/oncotarget.7709
- Nayak, S., Blumenfeld, N.R., Laksanasopin, T., Sia, S.K., 2017. Point-of-Care Diagnostics: Recent Developments in a Connected Age. *Anal. Chem.* 89, 102–

123. doi:10.1021/acs.analchem.6b04630

- Orozco, J., Suárez, G., Fernández-Sánchez, C., McNeil, C., Jiménez-Jorquera, C., 2007. Characterization of ultramicroelectrode arrays combining electrochemical techniques and optical microscopy imaging. *Electrochim. Acta* 53, 729–736. doi:10.1016/j.electacta.2007.07.049
- Patterson, C.C., Harjutsalo, V., Rosenbauer, J., Neu, A., Cinek, O., Skriverhaug, T., Rami-Merhar, B., Soltesz, G., Svensson, J., Parslow, R.C., Castell, C., Schoenle, E.J., Bingley, P.J., Dahlquist, G., Jarosz-Chobot, P.K., Marčiulionytė, D., Roche, E.F., Rothe, U., Bratina, N., Ionescu-Tirgoviste, C., Weets, I., Kocova, M., Cherubini, V., Rojnic Putarek, N., deBeaufort, C.E., Samardzic, M., Green, A., 2018. Trends and cyclical variation in the incidence of childhood type 1 diabetes in 26 European centres in the 25 year period 1989-2013: a multicentre prospective registration study. *Diabetologia*. doi:10.1007/s00125-018-4763-3
- Perry, D.J., Fitzmaurice, D.A., Kitchen, S., MacKie, I.J., Mallett, S., 2010. Point-of-care testing in haemostasis. *Br. J. Haematol.* 150, 501–514. doi:10.1111/j.1365-2141.2010.08223.x
- Shadfan, B.H., Simmons, A.R., Simmons, G.W., Ho, A., Wong, J., Lu, K.H., Bast, R.C., McDevitt, J.T., 2015. A multiplexable, microfluidic platform for the rapid quantitation of a biomarker panel for early ovarian cancer detection at the point-of-care. *Cancer Prev. Res.* 8, 37–48. doi:10.1158/1940-6207.CAPR-14-0248
- Shafiee, H., Wang, S., Inci, F., Toy, M., Henrich, T.J., Kuritzkes, D.R., Demirci, U., 2015. Emerging Technologies for Point-of-Care Management of HIV Infection. *Annu. Rev. Med.* 66, 387–405. doi:10.1146/annurev-med-092112-143017
- Shen, F., Du, W., Davydova, E.K., Karymov, M.A., Pandey, J., Ismagilov, R.F., 2010. Nanoliter multiplex pcr arrays on a slipchip. *Anal. Chem.* 82, 4606–4612. doi:10.1021/ac1007249
- Silva, D. Da, Zancan, P., Coelho, W.S., Gomez, L.S., Sola-Penna, M., 2010. Metformin reverses hexokinase and 6-phosphofructo-1-kinase inhibition in skeletal muscle,

- liver and adipose tissues from streptozotocin-induced diabetic mouse. *Arch. Biochem. Biophys.* 496, 53–60. doi:10.1016/j.abb.2010.01.013
- Sireci, A.N., 2015. Hematology Testing in Urgent Care and Resource-Poor Settings. An Overview of Point of Care and Satellite Testing. *Clin. Lab. Med.* 35, 197–207. doi:10.1016/j.cll.2014.10.009
- Tian, T., Wei, X., Jia, S., Zhang, R., Li, J., Zhu, Z., Zhang, H., Ma, Y., Lin, Z., Yang, C.J., 2016. Integration of target responsive hydrogel with cascaded enzymatic reactions and microfluidic paper-based analytic devices ( $\mu$ PADs) for point-of-care testing (POCT). *Biosens. Bioelectron.* 77, 537–542. doi:10.1016/j.bios.2015.09.049
- Tuttle, R., Weick, A., Schwarz, W.S., Chen, X., Obermeier, P., Seeber, L., Tief, F., Muehlhans, S., Karsch, K., Peiser, C., Duwe, S., Schweiger, B., Rath, B., 2015. Evaluation of novel second-generation RSV and influenza rapid tests at the point of care. *Diagn. Microbiol. Infect. Dis.* 81, 171–176. doi:10.1016/j.diagmicrobio.2014.11.013
- Wang, Y., Wang, W., Yu, L., Tu, L., Feng, Y., Klein, T., Wang, J.P., 2015. Giant magnetoresistive-based biosensing probe station system for multiplex protein assays. *Biosens. Bioelectron.* 70, 61–68. doi:10.1016/j.bios.2015.03.011
- Yoo, E.H., Lee, S.Y., 2010. Glucose biosensors: An overview of use in clinical practice. *Sensors* 10, 4558–4576. doi:10.3390/s100504558
- Zarkadas, G.M., Stergiou, A., Papanastasiou, G., 2001. Influence of tartaric acid on the electrodeposition of silver from binary water + dioxane AgNO<sub>3</sub>solutions. *J. Appl. Electrochem.* 31, 1251–1259. doi:10.1023/A:1012780022283



## Figure Captions

**Figure 1. Device scheme and picture of mobile application, device and  $\mu$ Potentiostat.** Main parts of the device depicted in assembly order from bottom to top (a-e). PMMA made pieces (a, c and e) represent the base (holding the silicon based electrodes array), channel-chamber and cover parts respectively. PDMS layers (b and d) are introduced among the channel-chamber and the other two pieces to avoid any leakage. On the bottom (f), the whole device from a top view. On the right side, a picture of the three independent elements for the measurement: mobile phone with the controlling application, PMMA-PDMS device and  $\mu$ Potentiostat circuit.

**Figure 2. Membranes electrodeposition and multi-analyte detection cycle.** Top view of closed chamber with a four electrodes chip: a) empty, b) chamber filled with alginate precursor for glucose detection 1, c) hydrogel electrodeposition, d) chamber rinsing to eliminate first precursor excess, e) chamber filled with alginate precursor for lactate detection, f) chamber rinsing to eliminate second precursor excess, g) colour change result of the reaction that occurs in the membrane with glucose, h) colour change result of the reaction that occurs in the membrane with lactate. Finally, the chamber is washed with PBS to dissolve the membranes.

**Figure 3. Real sample measurement scheme.** PMMA-PDMS construction including the open-closed system for the top block. In the electrodeposition mode a), the gate remains closed, while the alginate membrane is electrodeposited. For real sample analysis b), the gate is open and a drop of blood is added. Once the measurement is finished, the gate is closed again and the chamber is cleaned with PBS. Calibrations of spiked blood samples are depicted in c) for glucose and d) for lactate (n=5). Used blood had an initial content of 2 mM lactate and 4 mM glucose. TMB stock solution is added to the samples to a final TMB concentration of 2 mM prior to detection.

**Figure 4. Calibration and cross-talk analysis.** Calibration curves for a) glucose and b) lactate detection in FBS spiked samples (n=5). Response to glucose and lactate when GOx or LOx are present or absent in the gel precursor. Only when both enzymes are present in the respective hydrogel, two signals are obtained proportionally to glucose and lactate concentrations (WE1 and WE2 respectively). When any of the enzymes is not present (or both) the signal for the specific analyte is negligible. FBS had an initial content of 2 mM lactate and 4 mM glucose. TMB stock solution is added to the samples to a final TMB concentration of 2 mM prior to detection.

**Figure 5. Animals' samples comparison.** Plasma glucose a) and lactate c) in control and streptozotocin-induced diabetic mice. Glycaemia was significantly increased in diabetic mice whereas plasma lactate concentration was decreased compared to control non-diabetic mice. Data are expressed as mean  $\pm$  SEM (n=5-6). \*\*P<0.01, \*\*\*P<0.001 vs CT group (t-test). In b) and d), results obtained with the Automated Clinical Chemistry Analyzer Olympus AU480 (\*) in the determination of glucose and lactate were compared to the ones obtained with the device.

Figure 1.

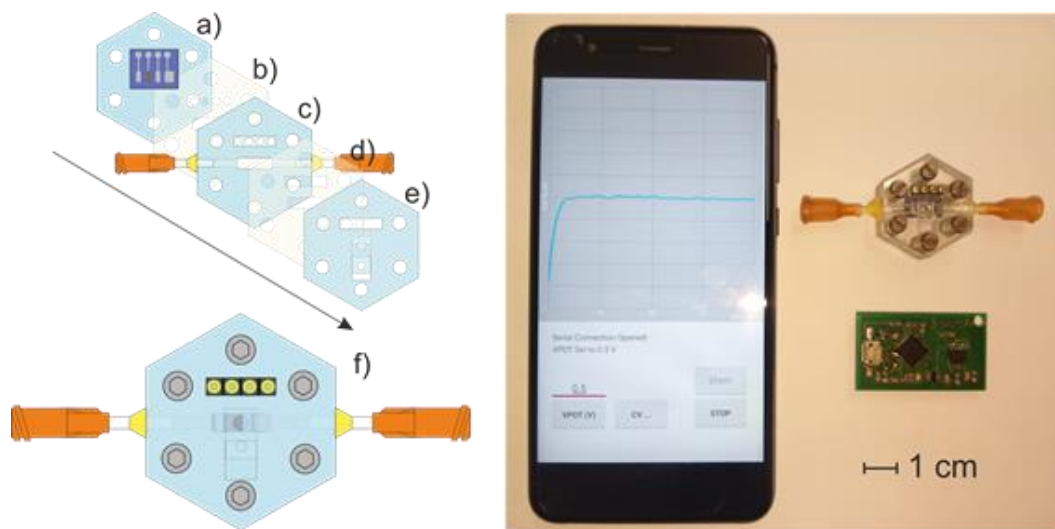
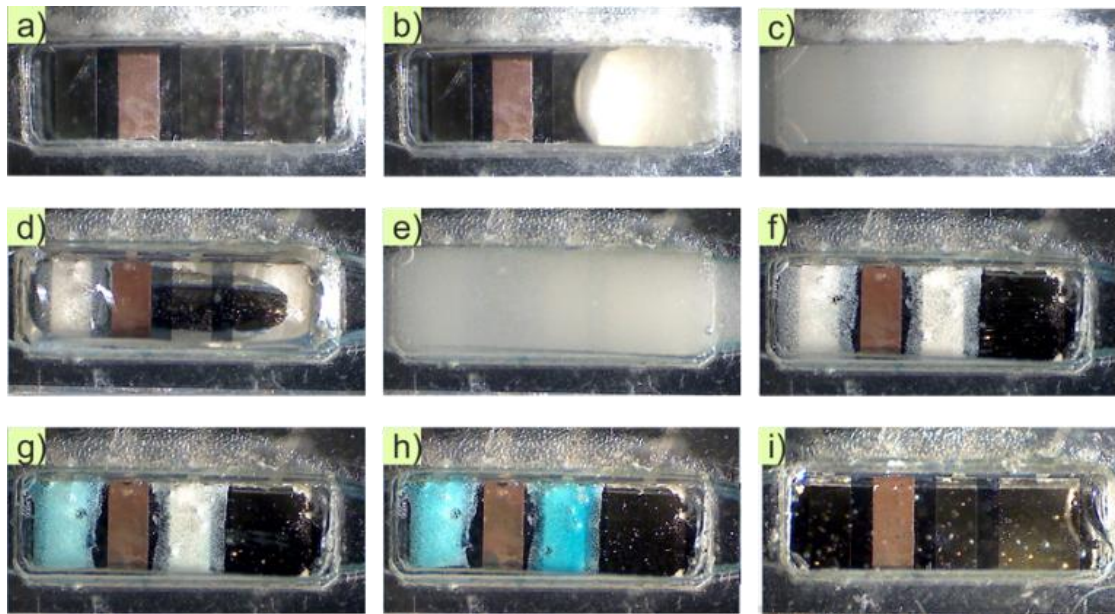
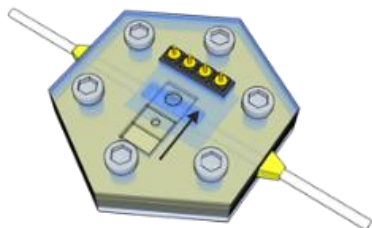


Figure 2.



**Figure 3.**

a) Electrodeposition mode



a.1) Hydrogel precursor injection



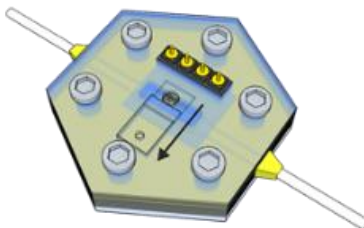
a.2) Hydrogels formation



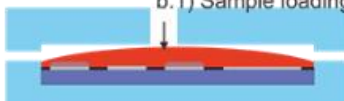
a.3) Chamber rinsing



b) Measurement mode



b.1) Sample loading



b.2) Detection



b.3) Membranes removal

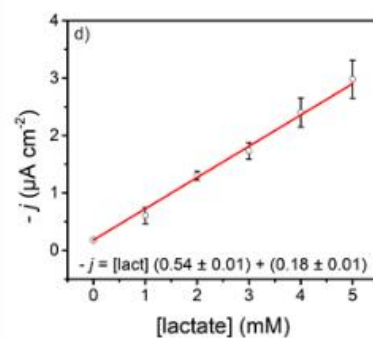
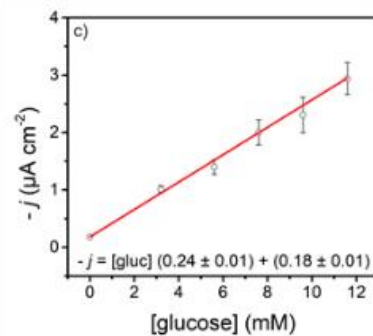


Figure 4.

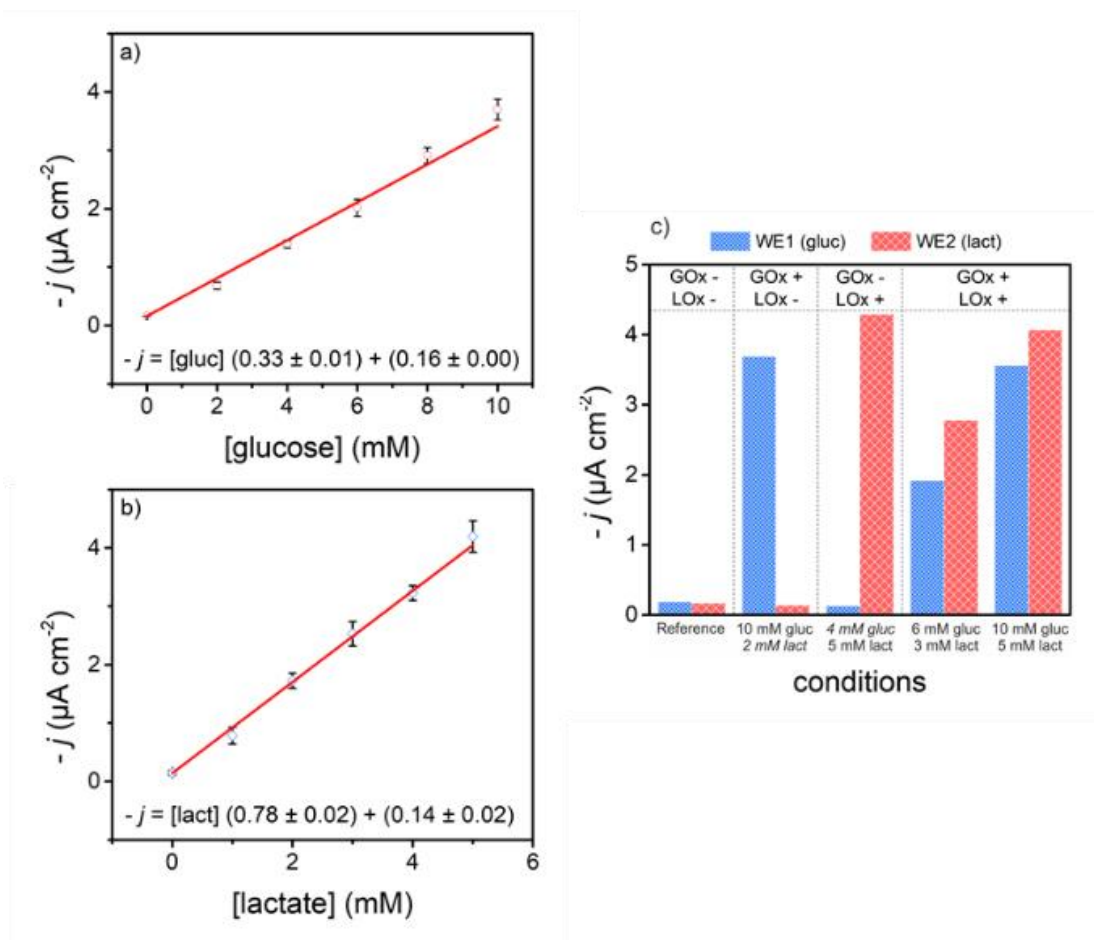


Figure 5.

